

MAGNETORESISTIVE PROPERTIES OF DIRAC SEMIMETAL Cd_3As_2 FERROMAGNETIC SEMICONDUCTOR AT HIGH PRESSURE

M.M. GADJIALIEV, L.A. SAIPULAEVA, A.G. ALIBEKOV, A.YU. MOLLAEV,
V.S. ZAKHVALINSKY, S.F. MARENKIN, T.N. EFENDIEVA

*Amirhanov Institute of Physics, Dagestan Scientific Centre,
Russian Academy of Sciences, 367003 Makhachkala, Russia*

The composite samples of $\text{Cd}_3\text{As}_2+\text{MnAs}$ (MnAs – 20 mole per cent) are prepared. We investigate the structure of samples using the X-ray powder diffraction, differential thermal, and energy dispersive analyses. The research of electric and magnetic properties of $\text{Cd}_3\text{As}_2+\text{MnAs}$ (MnAs – 20 mole per cent) under high hydrostatic pressure reveals that the phase transitions appear on pressure dependences of the resistivity and the Hall coefficient. Pressure-induced negative magnetoresistance is observed on magnetic-field dependences.

Keywords: composite, ferromagnetic semiconductor, hall effect, magnetoresistance, magnetoresistive properties.

PACS: 61.82.Fk, 62.23.Pq, 62.50.P

INTRODUCTION

A crucial problem is preparation of Cd_3As_2 - based ferromagnetic semiconductors [1, 4, 5]. For instance, Cd_3As_2 with Cr provided the suppression of near zero effective mass ultra-relativistic states at the substitution of Cr atoms for Cd [6].

Manganese dissolves in Cd_3As_2 forming a wide region of triple solid solutions $(\text{Cd}_{1-x}\text{Mn}_x)_3\text{As}_2$. An increase in Mn-content results in formation of Cd_3As_2 – based composite containing MnAs inclusions along with $\text{Cd}_{1-x}\text{Mn}_x)_3\text{As}_2$ solid solution. The MnAs ferromagnetic phase crystallizes on a hexagonal lattice P63/mmc with unit cell parameters $a=3.72$ Å and $c=5.71$ Å. The hexagonal structure of NiAs-type P63/mmc symmetry in MnAs changes to orthorhombic structure of MnP-type Pnma symmetry at room temperature with increasing the pressure up to 0.45 GPa [7].

MnAs compound possesses the ferromagnetism with a Curie temperature 318 K. This makes it a promising material for different elements of the spin electronics operating in a terahertz range [8,9,10]. Solid solutions of diluted magnetic semiconductors $(\text{Cd}_{1-x}\text{Mn}_x)_3\text{As}_2$ possess InSb-type band structure; the forbidden band width at low temperatures follows the linear dependence $E_0 = -0.095+1.45x$ (x is the Mn concentration) [11]. The band structure of Cd_3As_2 semiconductor is studied for long period of time and in series of works the band inversion along with the gapless-state is suggested [12]. The evolution of bands in Cd_3As_2 - based ternary and quaternary solid solutions is attractive as a separate problem [13] and enlightens the understanding of Cd_3As_2 properties as 3D Dirac semimetal [1]. The study of physical parameters dependence of Cd_3As_2 – MnAs system on a composition and pressure allows us to determine the points of Dirac semimetal (DSM) and semiconductor phase transition.

For the first time, in this work we perform complex researches of $\text{Cd}_3\text{As}_2+\text{MnAs}$ crystal structure, MnAs – 20 mole per cent, and an influence of the temperature, magnetic field, and pressure on the charge transport.

METHOD AND TECHNIQUE

The hydrostatic pressure $P \leq 9$ GPa was produced in a toroid-type device improved in such a way as to perform simultaneous measurements for few kinetic coefficients. For the purpose of simultaneous measuring the resistivity, Hall effect, and magnetoresistance, we used a multiturn solenoid allowing for generating the magnetic field of $H \leq 5$ kOe. A fluoroplastic cell of ~ 80 mm³ fitted with 12 electric contacts was used for measuring the resistivity and the Hall effect and pressure control at compression and decompression. A manganin manometer was graduated against Bi, Ti, and other standards. The parallelepiped samples had sizes of $2.8 \times 0.7 \times 0.5$ mm. As a pressure transmitting medium, we used ethanol and methanol mixture (4:1), which is hydrostatic up to 10 GPa. The electrical contacts were made by tin-based solders. The uncertainties in the resistivity, Hall effect, and pressure measurements didn't exceed ± 3 , 3.5, and 3 per cents, respectively. A detailed description of the method is presented in [14, 15].

RESULTS AND DISCUSSION

We research the structure of a ferromagnetic semiconductor of $\text{Cd}_3\text{As}_2+\text{MnAs}$ (MnAs – 20 mole per cent) at room temperature by means of PDA, DTA, the energy dispersive analysis (EDA), scanning electron and optical microscopy, and the Raman spectroscopy. The Hall effect, resistivity, and magnetoresistance measurements are performed under hydrostatic pressure up to 9 GPa at room temperatures. Figure 1 depicts the PDA results for $\text{Cd}_3\text{As}_2+\text{MnAs}$ (MnAs – 20 mole per cent). The line diagram of powder pattern shows that the crystal is composite, with prevailed α' -phase of Cd_3As_2 . Previously, Pietraszko, Lukaszewicz [16] reported that relatively high crystallization rates used at the Cd_3As_2 synthesis can be responsible for few inclusions of high-temperature phases of that at room temperature. The same is observed for heavily doped samples, for instance, in $\text{Cd}_3\text{As}_2+\text{MnAs}$ both α' - Cd_3As_2 and α'' - Cd_3As_2 phases were revealed [17]. The diffraction peak for magnetic MnAs phase is clearly determined only in the (101) plane

(Fig. 1) that was confirmed by the scanning electron microscopy (SEM) (see below). Dashed diagrams stand for different polymorphous modifications of cadmium arsenide.

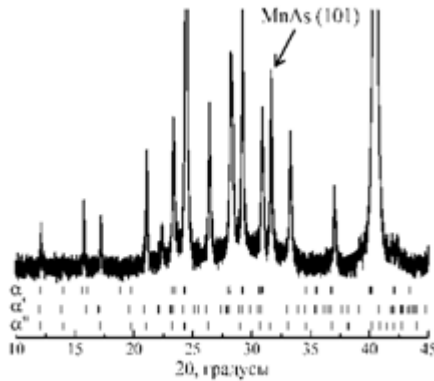


Fig. 1. X-ray patterns of Cd_3As_2+20 modifications of cadmium arsenide.

The multiphase composition of samples was confirmed when investigating the surfaces by SEM and the confocal microscopy (CM) (Fig. 2).

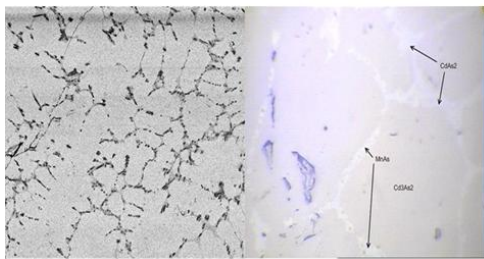


Fig. 2. The SEM (left inset) and confocal microscopy (right inset) images of Cd_3As_2+20 mole per cent MnAs sample.

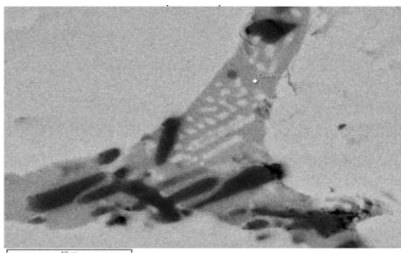


Fig. 3. The enlarged segment of the microstructure pictured in Fig. 2 (left) presents the images of Cd_3As_2+MnAs (MnAs – 20 mole per cent) surface.

The greater part of the sample is homogeneous that, according to the elemental analysis, is corresponded to Cd_3As_2 . Additional inclusions occupy less than 5 per cent of a sample surface area, in which the content of arsenic is higher than cadmium as opposed to the main sample bulk. An enlarged segment of the image (Fig. 2 (left) and Fig.3) clearly displays a complex nature of the inclusion, which in turn contains submicron inclusions similar in composition to Cd_3As_2 . The elemental analysis in a dark area of the inclusion shows a second phase to be $CdAs_2$. Since the grown samples are the polycrystals, the

inclusions, apparently, are the eutectic composition of $Cd_3As_2 - CdAs_2$ on the Cd_3As_2 crystallite boundaries. The spreading of manganese in the sample at the submicron level is homogeneous. That means, a part of Mn is dissolved in Cd_3As_2 matrix and, besides the $Cd_3As_2 - CdAs_2$ eutectics, the Mn inclusions are found on crystallite boundaries and don't exceed micrometer dimensions, according to PDA (Fig. 1).

In Fig. 4, we show differential thermal analysis of $Cd_3As_2 + MnAs$ samples. The DTA results for 80 mole per cent $Cd_3As_2 - 20$ mole per cent MnAs are interpreted as follows: 584 °C is the temperature of polymorphous transformation $\alpha \rightarrow \beta$ Cd_3As_2 ; 610°C is the melting point of the eutectics; 713 °C is the liquidus point.

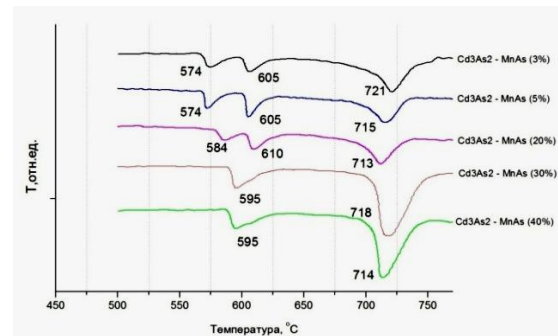


Fig. 4. DTA results of $Cd_3As_2 + MnAs$ samples.

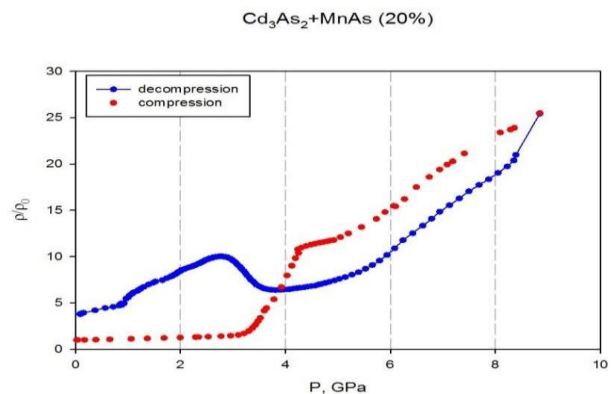


Fig. 5. The resistivity versus pressure curve for Cd_3As_2+20 mole per cent MnAs under MnAs.

The pressure measurements results for the resistivity, Hall coefficient, and magnetoresistance are depicted in Figs 5,6,7. The pressure dependence of the resistivity and Hall coefficient in Cd_3As_2+MnAs (MnAs – 20 mole per cent) is illustrated in Figs 6, 7.

With increasing the pressure, the resistivity doesn't change up to $P \approx 2.8$ GPa, after that it sharply rises (approximately by a factor of 12) achieving a maximum at $P=4.2$ GPa (Fig. 5). When decreasing the pressure, it drops with different baric coefficients and gains a maximum at $P=2.75$ GPa. The discrepancies in resistivity values before and after pressure application can be associated with the structure of the composite or with a probable second phase transition under $P > 8$, a nature of which needs a further analysis.

The dependence the Hall coefficient $R_H(P)$ on the pressure is illustrated in Fig. 6. The Hall coefficient passes through a maximum up to $P \approx 3.65$ GPa (Fig. 6).

The Hall coefficient versus pressure curve correlates well with the pressure dependence of $\rho(P)$, which also has a clear peak.

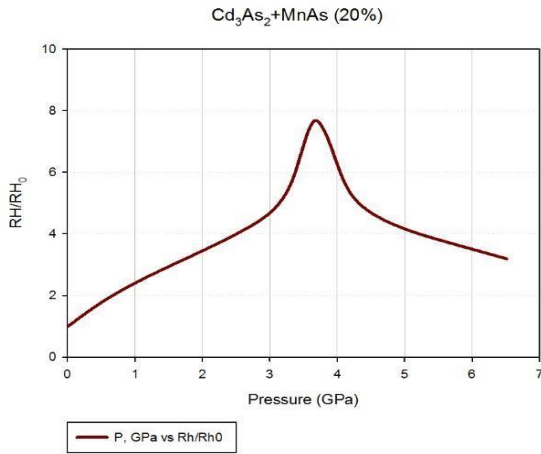


Fig. 6. The pressure dependence of the Hall coefficient for Cd_3As_2+20 mole per cent compression and decompression.

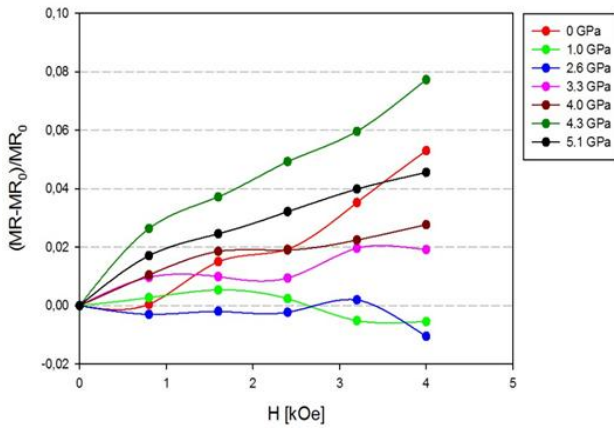


Fig. 7. magnetic field dependence of the magnetoresistivity under fixed pressures.

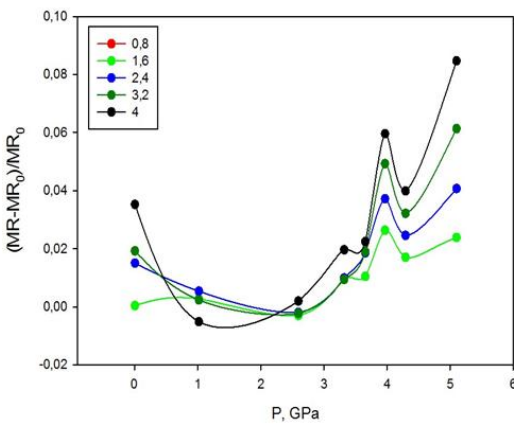


Fig. 8. The pressure dependence of the magnetoresistivity under fixed pressures.

The magnetic field dependence of the magnetoresistance under fixed pressures of $P \approx 0 \div 5.1$ GPa for Cd_3As_2+MnAs (MnAs–20 mole per cent) is

shown in Fig. 7. The magnetoresistance, positive at zero pressure, is suppressed with increasing the pressure. Starting from $P \approx 1$ GPa and $P \approx 2.6$ GPa, it drops achieving maxima, which shift towards high magnetic fields with raising the pressure.

The magnetoresistance versus pressure curves in Fig. 8. demonstrate a phase transition emerged at $P \approx 4$ GPa, a value of which, on a high pressure scale, agrees with phase transition values on $\rho(P)/\rho_0(P)$ and $R_h(P)/R_{h0}(P)$ curves in Figs 5, 6. The value of the transition maximum on the magnetoresistance versus pressure curve rises with growth in a magnetic field intensity.

CONCLUSION

The values of phase transitions emerged on pressure dependences of the resistivity, Hall coefficient, and magnetoresistance under high pressure agree well with phase transition values on $\rho(P)/\rho_0(P)$ and $R(P)/R_0(P)$ curves. Such a good agreement of experimental pressure dependences can be interpreted by a spin-reorientation magnetic phase transition in intermetallic compound of MnAs resulting from a change in structure parameters under high pressures. It is known, that magnetic and structural properties of MnAs and alloys are closely related [15]. The technology of Cd_3As_2+MnAs (MnAs–20 mole per cent) synthesis leads to the generation of granular structures (composite), which is a semiconducting (non-magnetic) matrix with ferromagnetic nanoclusters. In Ref. [18], the spin-reorientation transitions in MnAs were revealed on exposure to high pressure. It was determined that the position of manganese atoms in the magnetic cell (by additional superstructure magnetic reflex) at $P=3.8$ GPa can be described by space group $P21/c$. In ferromagnetic hexagonal MnAs structure under normal pressure and $T_c = 318$ K, the manganese atoms form layers perpendicular to a axis. Manganese nearest neighbor magnetic exchange interactions at 2.85 \AA range in adjacent layers are dominant, while Mn next-to-nearest neighbor interactions inside the layers at about 3.7 \AA range are noticeably weaker. The structural changes induced by hexagonal-to-orthorhombic transition have a little effect on a distance between nearest neighbors, that is about 2.81 \AA at $P = 3.8$ GPa, however, the ranges between next-to-nearest neighbors substantially change to about $2.98, 3.39, 4.43 \text{ \AA}$ at the same pressure. Thus, the observed magnetic phase transition can be explained within the framework of the Kittel model [19] due to the change in sign of Mn next-to-nearest neighbor exchange interactions under compression [20]. Basing on the data of works [2, 3, 20, 21] and our measurements, we can suggest that two phase transitions in Cd_3As_2 and MnAs, emerged in Cd_3As_2+MnAs (MnAs–20 mole per cent) nanocomposite under high pressure, influence on the carrier transport and the magnetoresistance. The composite matrix is solid $(Cd_{1-x}Mn_x)_3As_2$ due to the subsolution of manganese. The matrix of narrow gap semiconductor and structural phase transition Cd_3As_2 and the spin-reorientation magnetic transition in MnAs nanoclusters contribute to the pressure dependence of the magnetoresistance of Cd_3As_2+MnAs (MnAs–20 mole per cent).

- [1] A.V. Galeeva, I.V. Krylov, K.A. Drozdov, A.F. Knjazev, A.V. Kochura, A.P. Kuzmenko, V.S. Zakhvalinskii, S.N. Danilov, L.I. Ryabova, D.R. Khokhlov. Electron energy relaxation under terahertz excitation in $(\text{Cd}_{1-x}\text{Zn}_x)_3\text{As}_2$ Dirac semimetals *Bellstein J. Nanotechnol.* 8 (2017) 167.
- [2] Lampo He, YatingJia, Sijia Zhang, Xiaochen Hong, Changqing Jin and Shiyang Li. Pressureinduced superconductivity in the three-dimensional topological Dirac semimetal Cd_3As_2 , *npj Quantum Materials*, 1 (2016) 16014.
- [3] S. Zhang, et al. Breakdown of three-dimensional Dirac semimetal state in pressurized Cd_3As_2 . *Phys. Rev. B* 91, 165133 (2015).
- [4] E.K. Arushanov. II_3V_2 Compounds and Alloys, *Prog. Crystal Growth and Charact.* 1992, Vol. 25, pp. 131-201.
- [5] J. Cisowski. Semimagnetic Semiconductors Based on II-V Compounds, *Phys. Stat. Sol. (b)* 200, 311 (1997).
- [6] X. Yuan, P. Cheng, L. Zhang, Ch. Zhang, J. Wang, Y. Liu, Q. Sun, P. Zhou, D.W. Zhang, Z. Hu, X. Wan, H. Yan, Z. Li, F. Xiu. Direct observation of Landau level resonance and mass generation in Dirac semimetal Cd_3As_2 thin films *Nano Letters*. 17 (2017) 2211.
- [7] I.F. Gribanov, E.A. Zavadsky, A.P. Sivachenko. The low-temperature transformations in orthorhombic arsenide manganese. *Fiz. Nizkh. Temp.*, 1979, v. 5, pp.1219-1223. (1979).
- [8] C. Spezzani, E. Ferrari, E. Allaria, F. Vidal, A. Ciavardini et al. Magnetization and Microstructure Dynamics in Fe/MnAs/GaAs (001): Fe Magnetization Reversal by a Femtosecond Laser Pulse *Physical Review Letters*. 2014. V. 113. Iss. 24. P. 247202.
- [9] J. Hubmann, B. Bauer, H.S. Korner, S. Furthmeier, M. Buchner, G. Bayreuther et al. Epitaxial Growth of Room-Temperature Ferromagnetic MnAs Segments on GaAs Nanowires via Sequential Crystallization *Nano Letters*. 2016. V. 16. iss. 2. p. 900-905.
- [10] V.M. Novotortsev, S.F. Marenkin, I.V. Fedorchenko, A.V. Kochura. Physicochemical Foundations of Synthesis of New Ferromagnets from Chalcopyrites $\text{A}^{\text{II}}\text{B}^{\text{IV}}\text{C}^{\text{V}}_2$. *Russian Journal of Inorganic Chemistry*. 2010. V. 55. No.11. P. 1762-1773.
- [11] M.J. Aubin, L.G. Caron and J.-P. Jay-Gerin. Band structure of cadmium arsenide at room temperature, *Phys. Rev B*. 15, (1977) p.p.3872-3878.
- [12] R.J. Wagner, E.D. Palik, and E.M. Swiggard. In *Physics of Semimetals and Narrow-Gap Semiconductors* D.L. Carter and R.T. Bate, eds.), p.471. Pergamon, New York, 1971.
- [13] E.K. Arushanov, A.F. Knyazev, A.N. Nateprov, S.I. Radautsan. Composition Dependence of the Energy Gap in $\text{Cd}_3\text{-xZn}_x\text{As}_2$ *Fiz. Tekh. Poluprovodn.*, 1983, v.17, N7, pp.1202-1204.
- [14] A.Yu. Mollaev, L.A. Saipulaeva, R.K. Arslanov, S.F. Marenkin. Effect of hydrostatic pressure on the transport properties of cadmium diarsenide crystals. *Inorganic Materials*. 2001. V. 37. № 4. P. 327-330.
- [15] L.G. Khvostantsev, L.P. Vereshchagin, A.P. Novikov. *High Temperatures - High Pressures*. 1977. V. 9. № 6. p. 637.
- [16] A. Pietraszko, K. Lukaszewicz. Thermal Expansion and Phase Transitions of Cd_3As_2 and Zn_3As_2 . *Phys. Stat. Sol. (a)*. 1973. V. 18. P. 723.
- [17] A.I. Ril, A.V. Kochura, S.F. Marenkin, A.E. Kuzko, B.A. Aronzon. Crystall Microstructure of $\text{Cd}_3\text{As}_2 - \text{MnAs}$ system, *Proceeding of Southwest State University. Technics and Technologies*, 2017, vol. 7, no. 2(23), pp. 120-134.
- [18] S.K. Asadov, E.A. Zavadskii, V.I. Kamenev, E.P. Stefanovskii, A.L. Sukstanskii, B.M. Todris. Relation of Magnetic and Structural Factors in the Course of Phase Transitions in MnAs- Based Alloys, *Physics of the Solid State*, 2000, Volume 42, issue 9, pp 1696-1704.
- [19] C. Kittel. Model of exchange-inversion magnetization. *Phys. Rev.* -1960. -V. 120. -P. 335-342.
- [20] D.P. Kozlenko. Magnetic and orientational ordering in systems with competing interactions at high pressures: dis ... Doctor of Physical and Mathematical Sciences, Yekaterinburg, 2008. 350.
- [21] A.D. Izotov, V.P. Sanygin, V.F. Ponomarev. Genetic relation between crystal structures of polymorphic modifications of $\text{A}^{\text{II}}\text{B}^{\text{V}}$ - type compounds. *Crystallography*, 1978, 23, 767. (1978)

Received: 02.04.2018